



Universiteit
Leiden
The Netherlands

Tracer-based lipidomics enables the discovery of disease-specific candidate biomarkers in mitochondrial β -oxidation disorders

Schwantje, M.; Mosegaard, S.; Knottnerus, S.J.G.; Klinken, J.B. van; Wanders, R.J.; Lenthe, H. van; ... ; Vaz, F.M.

Citation

Schwantje, M., Mosegaard, S., Knottnerus, S. J. G., Klinken, J. B. van, Wanders, R. J., Lenthe, H. van, ... Vaz, F. M. (2024). Tracer-based lipidomics enables the discovery of disease-specific candidate biomarkers in mitochondrial β -oxidation disorders. *The Faseb Journal*, 38(4). doi:10.1096/fj.202302163R

Version: Publisher's Version







License: [Creative Commons CC BY 4.0 license](#)

Downloaded from: <https://hdl.handle.net/1887/4195592>

Note: To cite this publication please use the final published version (if applicable).

RESEARCH ARTICLE

Tracer-based lipidomics enables the discovery of disease-specific candidate biomarkers in mitochondrial β -oxidation disorders

Marit Schwantje^{1,2}  | Signe Mosegaard^{1,3,4,5}  | Suzan J. G. Knottnerus^{1,3} |
Jan Bert van Klinken^{6,7} | Ronald J. Wanders^{1,3} | Henk van Lenthe¹ | Jill Hermans⁶ |
Lodewijk IJlst^{1,3} | Simone W. Denis¹ | Yorrick R. J. Jaspers^{1,6} | Sabine A. Fuchs²  |
Riekelt H. Houtkooper^{1,3,4,5}  | Sacha Ferdinandusse^{1,3}  | Frédéric M. Vaz^{1,3,5,6} 

¹Laboratory Genetic Metabolic Diseases, Department of Clinical Chemistry, Amsterdam UMC, University of Amsterdam, Amsterdam, the Netherlands

²Department of Metabolic Diseases, Wilhelmina Children's Hospital, University Medical Center Utrecht, Utrecht, the Netherlands

³Amsterdam Gastroenterology, Endocrinology, and Metabolism, Amsterdam, the Netherlands

⁴Amsterdam Cardiovascular Sciences, Amsterdam, the Netherlands

⁵Emma Center for Personalized Medicine, Amsterdam UMC, Amsterdam, the Netherlands

⁶Core Facility Metabolomics, Amsterdam UMC, University of Amsterdam, Amsterdam, the Netherlands

⁷Department of Human Genetics, Leiden University Medical Center, Leiden, the Netherlands

Abstract

Carnitine derivatives of disease-specific acyl-CoAs are the diagnostic hallmark for long-chain fatty acid β -oxidation disorders (lcFAOD), including carnitine shuttle deficiencies, very-long-chain acyl-CoA dehydrogenase deficiency (VLCADD), long-chain 3-hydroxyacyl-CoA dehydrogenase deficiency (LCHADD) and mitochondrial trifunctional protein deficiency (MPTD). The exact consequence of accumulating lcFAO-intermediates and their influence on cellular lipid homeostasis is, however, still unknown. To investigate the fate and cellular effects of the accumulating lcFAO-intermediates and to explore the presence of disease-specific markers, we used tracer-based lipidomics with deuterium-labeled oleic acid (D₉-C18:1) in lcFAOD patient-derived fibroblasts. In line with previous studies, we observed a trend towards neutral lipid accumulation in lcFAOD. In addition, we detected a direct connection between the chain length and patterns of (un)saturation of accumulating acylcarnitines and the various enzyme deficiencies. Our results also identified two disease-specific candidate biomarkers. Lysophosphatidylcholine(14:1) (LPC(14:1)) was specifically increased in severe VLCADD compared to mild VLCADD and control samples. This was confirmed in plasma samples showing an inverse correlation with enzyme activity, which was better than the

Abbreviations: CACTD, carnitine–acylcarnitine translocase deficiency; CE, cholesterol esters; CPT1D, carnitine palmitoyltransferase 1 deficiency; CPT2D, carnitine palmitoyltransferase 2 deficiency; DG, diacylglycerols; FADS, fatty acid desaturase; lcFAOD, long-chain fatty acid β -oxidation disorders; LCHADD, long-chain 3-hydroxyacyl-CoA dehydrogenase deficiency; LCKATD, long-chain acyl-CoA thiolase deficiency; LPC, lysophosphatidylcholine; LPE, lysophosphatidylethanolamine; MPTD, mitochondrial trifunctional protein deficiency; NBS, newborn screening; PC, phosphatidylcholine; PE, phosphatidylethanolamine; RT, retention time; TG, triacylglycerols; TG(O), alkyl diacylglycerols; VLCADD, very-long-chain acyl-CoA dehydrogenase deficiency.

Marit Schwantje and Signe Mosegaard shared first authors.

Riekelt H. Houtkooper, Sacha Ferdinandusse and Frédéric M. Vaz shared last authors.

This is an open access article under the terms of the [Creative Commons Attribution](https://creativecommons.org/licenses/by/4.0/) License, which permits use, distribution and reproduction in any medium, provided the original work is properly cited.

© 2024 The Authors. *The FASEB Journal* published by Wiley Periodicals LLC on behalf of Federation of American Societies for Experimental Biology.

Correspondence

Riekelt H. Houtkooper, Laboratory Genetic Metabolic Diseases, Amsterdam UMC, University of Amsterdam, Meibergdreef 9, Amsterdam, the Netherlands. Email: r.h.houtkooper@amsterdamumc.nl

Funding information

Metakids/PNO Zorg, Grant/Award Number: 2019_087; Independent Research Fund Denmark, Grant/Award Number: 1057-00039B; NWO, Grant/Award Number: 91118006

classic diagnostic marker C14:1-carnitine. The second candidate biomarker was an unknown lipid class, which we identified as S-(3-hydroxyacyl)cysteamines. We hypothesized that these were degradation products of the CoA moiety of accumulating 3-hydroxyacyl-CoAs. S-(3-hydroxyacyl)cysteamines were significantly increased in LCHADD compared to controls and other lcFAOD, including MTPD. Our findings suggest extensive alternative lipid metabolism in lcFAOD and confirm that lcFAOD accumulate neutral lipid species. In addition, we present two disease-specific candidate biomarkers for VLCADD and LCHADD, that may have significant relevance for disease diagnosis, prognosis, and monitoring.

KEYWORDS

biomarkers, inborn errors, lipid metabolism, lipid metabolism disorders, lipidomics, lipolysis and fatty acids, lysophospholipids, mitochondria

1 | INTRODUCTION

Fatty acids are, together with glucose and amino acids, the main substrates used to maintain metabolic homeostasis. Especially during fasting and exercise, organs such as the liver, heart and skeletal muscle rely highly on mitochondrial long-chain fatty acid β -oxidation (lcFAO) for energy production.¹ In addition to the generation of adenosine triphosphate (ATP) via the citric acid cycle and respiratory chain, fatty acids and their degradation products are important building blocks for the biosynthesis of different (macro)molecules.^{2,3}

Deficiency of any of the enzymes of the mitochondrial lcFAO system leads to impaired degradation of fatty acids and energy shortage. This group of inherited metabolic diseases are called the long-chain fatty acid β -oxidation disorders (lcFAOD) and comprise seven different disorders^{4,5}; carnitine palmitoyltransferase 1 deficiency (CPT1D), carnitine-acylcarnitine translocase deficiency (CACTD), carnitine palmitoyltransferase 2 deficiency (CPT2D), very long-chain acyl-CoA dehydrogenase deficiency (VLCADD) and deficiencies of the mitochondrial trifunctional protein (MTP) including generalized MTP deficiency (MTPD), long-chain 3-hydroxyacyl-CoA dehydrogenase deficiency (LCHADD) and long-chain acyl-CoA thiolase deficiency (LCKATD). The worldwide incidence of lcFAOD is highly variable between countries and ethnicities (ranging from 0.002% to 1.4%), and depends on, among others, the presence of NBS and specific variants in the population.⁶ lcFAOD can present with cardiomyopathy, rhabdomyolysis, hypoglycemia and for LCHADD/MTPD also with peripheral neuropathy and/or pigmentary retinopathy.⁴

Biochemically, lcFAOD are characterized by the accumulation of disease-specific acyl-CoAs, reflecting the enzyme deficiency. Measurement of concomitantly accumulating acylcarnitines¹ in plasma/blood spots is a well-established

and cheap diagnostic tool that also allows newborn screening (NBS) for lcFAOD, as implemented in many countries worldwide. The clinical spectrum of patients with lcFAOD detected through NBS is highly variable, ranging from severe neonatal and fatal disease, to mild myopathic and even asymptomatic phenotypes.⁷ It remains difficult to predict the clinical phenotype after diagnosis through NBS, complicating clinical decision-making and patient care. In recent years, measurement of lcFAO flux in fibroblasts has been introduced as a reliable disease severity marker for lcFAOD.⁸ Unfortunately, the lcFAO flux assay is only performed in a limited number of laboratories worldwide and requires a skin biopsy followed by fibroblast culturing, making this assay laborious and limited to only a small number of patients.

Although the acylcarnitine pattern is the diagnostic hallmark for lcFAOD, the exact role of the accumulation of lcFAO-intermediates in the pathophysiology of lcFAOD is largely unknown. It is hypothesized that certain accumulating lcFAO-intermediates may have toxic effects on tissues and organs, which together with metabolic energy shortage lead to clinical symptoms.^{4,9} How the accumulation of lcFAO-intermediates influences cellular lipid homeostasis and development of symptoms is poorly understood. A number of studies have shown increased intracellular lipid accumulation in muscle fibers in muscle biopsies from patients with MTPD and VLCADD.^{10–13} Other studies in lcFAOD patient-derived skin fibroblasts, cardiomyocytes and stem cell-derived LCHADD retina cells indicate a selective rerouting of long-chain fatty acids (LCFAs) into triacylglycerols (TG).^{14–16} Alati et al,¹⁵ who reported the first lipidomic analyses in fibroblasts derived from patients with three different lcFAOD (CPT2D, LCHADD and VLCADD), proposed that the accumulation of specific acyl-CoAs leads to changes in the complex lipid profile of cells, which probably contributes to the clinical symptoms in lcFAOD patients.

In the present study, we used tracer-based lipidomics using deuterium-labeled oleic acid (D9-C18:1) to further explore the fate of accumulating LCFAs and lcFAO-intermediates in fibroblasts of four different lcFAOD, i.e., CPT2D, LCHADD, MTPD and VLCADD. We here report a direct correlation between the accumulation of specific lcFAO-intermediates and the various enzyme deficiencies and a more general accumulation of neutral lipid species including TG. Moreover, tracer-based lipidomics allowed for the discovery of two disease-specific candidate biomarkers, LPC(14:1) for VLCADD and S-(3-hydroxyacyl) cysteamines for LCHADD.

2 | MATERIALS AND METHODS

2.1 | Fibroblast culture

Skin fibroblasts from six healthy controls, three CPT2D patients, five LCHADD patients, three MTPD patients, six severe VLCADD patients (lcFAO flux $\leq 10\%$) and six mild VLCADD patients (lcFAO flux $> 10\%$) were included (Table 1). For the patient and control fibroblasts used for the tracer-based lipidomics, informed consent was obtained for research studies. Cells were cultured in Ham's F-10 medium (Gibco, cat. no. 11550043) supplemented with 10% fetal calf serum (Invitrogen) 25 mmol/L HEPES, 100 U/mL penicillin, 100 $\mu\text{g/mL}$ streptomycin, and 250 $\mu\text{g/mL}$ amphotericin in a humidified atmosphere of 5% CO_2 at 37°C. In parallel, all cell lines were cultured in the presence of a tracer, 50 μM D9-C18:1 (Avanti Polar Lipids, Cat. No. 8618090) and 25 $\mu\text{mol/L}$ LL-carnitine (Sigma-Aldrich, Cat. No. C0158). After 96 h of incubation, the fibroblasts were harvested by trypsinization and pellets were used for lipid isolation.

2.2 | Single-phase lipidomic extraction

Fibroblasts were resuspended in ultra-pure water and sonicated for 2×10 s at 8 W using a tip sonicator. For fibroblasts used to exclude extracellular formation of detected lipid clusters, methanol: chloroform and internal standards were added before sonication. The protein concentration of the homogenates was determined with the BCA assay¹⁷ and 250 μg of protein equivalent was used for lipid extraction. The lipid extraction was performed in a 2 mL tube with 1.5 mL internal standards dissolved methanol: chloroform (1:1 (v/v)) as previously described with minor changes.^{18,19} The following internal standards were added in listed quantities (per sample): bis(monoacylglycerol) phosphate (BMP)(14:0)₂ (0.2 nmol), ceramide-1-phosphate (C1P)(d18:1/12:0) (0.125 nmol), D7-cholesteryl

ester (CE) (16:0) (2.5 nmol), ceramide cer (d18:1/12:0) (0.125 nmol), ceramide cer (d18:1/25:0) (0.125 nmol), cardiolipin CL (14:0)₄ (0.1 nmol), diacylglycerol (DAG) (14:0)₂ (0.5 nmol), glucose ceramide GlcCer (d18:1/12:0) (0.125 nmol), lactose ceramide LacCer (d18:1/12:0) (0.125 nmol), lysophosphatidic acid LPA (14:0) (0.1 nmol), lysophosphatidylcholine LPC (14:0) (0.5 nmol), lysophosphatidylethanolamine (LPE) (14:0) (0.1 nmol), lysophosphatidylglycerol (LPG) (14:0) (0.02 nmol), phosphatidic acid (PA) (14:0)₂ (0.5 nmol), phosphatidylcholine (PC) (14:0)₂ (2 nmol), phosphatidylethanolamine (PE) (14:0)₂ (0.5 nmol), phosphatidylglycerol (PG) (14:0)₂ (0.1 nmol), phosphatidylinositol (PI) (8:0)₂ (0.5 nmol), phosphatidylserine (PS) (14:0)₂ (5 nmol), sphinganine 1-phosphate (S1P) (d17:0) (0.125 nmol), sphinganine-1-phosphate S1P(d17:1) (0.125 nmol), ceramide phosphocholines (SM) (d18:1/12:0) (2.125 nmol), sphingosine (SPH) (d17:0) (0.125 nmol), sphingosine (SPH) (d17:1) (0.125 nmol), and triacylglycerol (TG) (14:0)₃ (0.5 nmol). The mixture was thoroughly mixed and sonicated in a water bath for 5 min followed by centrifugation at 4°C (16 000 g for 5 min). The supernatant was transferred to a glass vial and evaporated under a stream of nitrogen at 60°C. The residue was dissolved in 150 μL of 1:1 (v/v) methanol: chloroform.

2.3 | Ultra-performance liquid chromatography-high-resolution mass spectrometry (UPLC-HRMS)

Lipids were analyzed using a Thermo Scientific Ultimate 3000 binary HPLC coupled to a Q Exactive Plus Orbitrap mass spectrometer. The normal phase separation of lipids was performed with 2 μL lipid extract that were injected on a Phenomenex, Luna 5 μm Silica 100 Å, 250 \times 2 mm maintained at 25°C. Mobile phase consisted of (A) 85:15 (v/v) methanol: water containing 0.025% formic acid and 6.7 mmol/L ammonia and (B) 97:3 (v/v) chloroform: methanol containing 0.025% formic acid. Using a flow rate of 0.3 mL/min, the LC gradient consisted of: Dwell at 10% A 0–1 min, ramp to 20% A at 4 min, ramp to 85% A at 12 min, ramp to 100% A at 12.1 min, dwell at 100% A 12.1–14 min, ramp to 10% A at 14.1 min, and dwell at 10% A for 14.1–15 min.

For reverse phase separation of lipids, 5 μL of lipid extract was injected onto an Acquity UPLC HSS T3 (100 \times 2.1 mm, 1.8 μm , Waters) maintained at 60°C. Mobile phase consisted of (A) 4:6 (v/v) methanol: water and B 1:9 (v/v) methanol: isopropanol, both containing 0.1% formic acid and 10 mmol/L ammonia. Using a flow rate of 0.4 mL/min, the LC gradient consisted of: Dwell at 100% A at 0 min, ramp to 80% A at 1 min, ramp to 0% A at 16 min, dwell at 0% A for 16–20 min, ramp to

TABLE 1 Patient cell lines characteristics.

CPT2D						
ID	Gene	Nucleotide change	Protein change	lcFAO flux ^a	Enzyme activity ^b	
					CPT2	Clinical phenotype
CPT2D_1	CPT2	c.[338C>T]; c.[370C>T]	p.Ser113Leu; p.Arg124Ter	NA	8.7%	Rhabdomyolysis, myoglobinuria, muscle pain from childhood onwards, exercise intolerance
CPT2D_2	CPT2	c.[338C>T]; c.[338C>T]	p.Ser113Leu; p.Ser113Leu	NA	18.2%	Rhabdomyolysis, myoglobinuria, muscle pain from adolescence onwards
CPT2D_3	CPT2	c.[338C>T]; c.[338C>T]	p.Ser113Leu; p.Ser113Leu	NA	23.3%	Myoglobinuria, muscle pain, suspected rhabdomyolysis, exercise intolerance
LCHADD						
ID	Gene	Nucleotide change	Protein change	lcFAO flux ^a	Enzyme activity ^b	
					LCHAD LCKAT	Clinical phenotype
LCHADD_1	HADHA	c.[1528G>C]; c.[1712T>C]	p.Glu510Gln; p.Leu571Pro	32	5.4% 37%	Rhabdomyolysis, symptomatic pigmentary retinopathy, mild peripheral neuropathy
LCHADD_2	HADHA	c.[1528G>C]; c.[2099delG]	p.Glu510Gln; p.Gly700GlufsX30	27	8.3% 43%	Illness induced rhabdomyolysis
LCHADD_3	HADHA	c.[1528G>C]; c.[1528G>C]	p.Glu510Gln; p.Glu510Gln	24	9.5% 138%	Exercise induced rhabdomyolysis, first signs of pigmentary retinopathy (asymptomatic) decreased Achilles tendon reflexes
LCHADD_4	HADHA	c.[1528G>C]; c.[1528G>C]	p.Glu510Gln; p.Glu510Gln	28	8.1% 104%	Exercise induced rhabdomyolysis, mild reversible cardiomyopathy and mild hypoglycaemia
LCHADD_5	HADHA	c.[1528G>C]; c.[1678C>T]	p.Glu510Gln; p.Arg560Ter	32	6.8% 31%	Rhabdomyolysis, pigmentary retinopathy, peripheral neuropathy, mild cardiomyopathy and hypoglycaemia at diagnosis
MTPD						
ID	Gene	Nucleotide change	Protein change	lcFAO flux ^a	Enzyme activity ^b	
					LCHAD LCKAT	Clinical phenotype
MTPD_1	HAHDA	c.[556C>G]; c.[1392+1G>A]	p.Gln186Glu; splicing defect	43	6.8% 2.4%	Severe rhabdomyolysis, severe impairing axonal sensorimotor neuropathy
MTPD_2	HADHA	c.[556C>G]; c.[1392+1G>A]	p.Gln186Glu; splicing defect	46	6.8% 2.4%	Severe rhabdomyolysis, severe impairing axonal sensorimotor neuropathy
MTPD_3	HADHB	c.[980T>C]; c.[209+1G>C]	p.Leu327Leu; splicing defect	40	16.2% 7.1%	Mild exercise intolerance, rhabdomyolysis, hypoparathyroidism, severe neuropathy with abnormal gait and muscle weakness

TABLE 1 (Continued)

VLCADD (severe)						
ID	Gene	Nucleotide change	Protein change	lcFAO flux ^a	Enzyme activity ^b	
					VLCAD	Clinical phenotype
SVLCADD_1	ACADVL	c.[1322G>A]; c.[1322G>A]	p.Gly441Asp; p.Gly441Asp	5	<5%	Rhabdomyolysis, hypoglycemia, cardiomyopathy (deceased)
SVLCADD_2	ACADVL	c.[643T>C]; c.[643T>C]	p.Cys215Arg; p.Cys215Arg	6	<5%	Rhabdomyolysis, hypoglycaemia
SVLCADD_3	ACADVL	c.[104delC]; c.[104delC]	p.Pro351LeufsX26; p.Pro351LeufsX26	6	<5%	Rhabdomyolysis
SVLCADD_4	ACADVL	c.[104delC]; c.[104delC]	p.Pro351LeufsX26; p.Pro351LeufsX26	7	<5%	Rhabdomyolysis, cardiomyopathy, hypoglycemia
SVLCADD_5	ACADVL	c.[1269+1G>A]; c.[1269+1G>A]	splicing defect	6	<5%	Rhabdomyolysis, cardiomyopathy, hypoglycemia
SVLCADD_6	ACADVL	c.[104delC]; c.[104delC]	p.Pro351LeufsX26; p.Pro351LeufsX26	6	<5%	Rhabdomyolysis, cardiomyopathy, hypoglycemia (deceased)
VLCADD (mild)						
ID	Gene	Nucleotide change	Protein change	lcFAO flux ^a	Enzyme activity ^b	
					VLCAD	Clinical phenotype
MVLCADD_1	ACADVL	c.[541dupC]; c.[1072A>G]	p.His181ProfsX72; p.Lys358Glu	51	9.5%	Exercise induced rhabdomyolysis
MVLCADD_2	ACADVL	c.[848T>C]; c.[1444_1448delAAGGA]	p.Val283Ala; p.Lys482AlafsX78	44	6.9%	Hypoglycemia
MVLCADD_3	ACADVL	c.[104delC]; c.[848T>C]	p.Pro351LeufsX26; p.Val283Ala	39	7.1%	Hypoglycemia and muscle pain
MVLCADD_4	ACADVL	c.[848T>C]; c.[848T>C]	p.Val283Ala; p.Val283Ala	78	11.4%	Asymptomatic
MVLCADD_5	ACADVL	c.[829_831delGAG]; c.[848T>C]	p.Glu277del; p.Val283Ala	127	19.2%	Asymptomatic
MVLCADD_6	ACADVL	c.[779C>T]; c.[848T>C]	p.Thr260Met; p.Val283Ala	37	<5%	Asymptomatic

Abbreviations: LCKAT, long-chain ketoacyl-CoA thiolase; NA, not analyzed.

^alcFAO flux was measured in fibroblasts and is calculated as % of the mean activity in the control fibroblasts analyzed in the same experiment. The cell lines were analyzed in two independent experiments and the measurements within the experiment were performed at least in duplicate.

^bEnzyme activity was measured in fibroblasts and the mean of technical duplicates was expressed as % of the mean of the reference range. Limit of quantitation of the VLCAD enzyme assay is 5% of the mean of the reference range.

100% A at 20.1 min, dwell at 100% A for 20.1–21 min. A Q Exactive Plus Orbitrap mass spectrometer (Thermo Fisher Scientific) was used in the negative and positive electrospray ionization mode using nitrogen as nebulizing gas. The spray voltage was 2500 V (neg) or 3500 V (pos), and the capillary temperature was 256°C. S-lens RF level: 50, auxiliary gas: 11, auxiliary gas temperature 300°C, Sheath gas: 48 au, Sweep cone gas: 2 au. Mass spectra of lipids were acquired in both scan modes by continuous scanning from m/z 150 to m/z 2000 with a resolution of 280 000 full width at half maximum (FWHM) and processed using an in-house developed lipidomics pipeline,²⁰ written in the R programming language (<http://www.r-project.org>). The identified peaks were normalized to the intensity of the internal standard for each lipid class.

2.4 | LPC(14:1) measurements in plasma

LPC(14:1) in plasma was analyzed using a Waters Acquity UPLC system coupled to a Waters Xevo TQ-S Micro mass spectrometer. The reversed phase separation was performed with 2 μ L of lipid extract that was injected on a Kinetex C8 LC Column (50 \times 2.1 mm, 2.6 μ m, Phenomenex) maintained at 50°C. Mobile phase consisted of (A) water containing 0.1% formic acid and (B) methanol containing 0.1% formic acid. Using a flow rate of 0.4 mL/min, the LC gradient consisted of a linear gradient from 50% A at 0 min to 100% B at 8.35 min, 100% B from 8.35 to 12.5 min, to 50% A at 12.6 min and equilibrate at 50% A from 12.6 to 14.5 min. The TQ-S Micro mass spectrometer (Waters) was used in the positive electrospray ionization mode using nitrogen as nebulizing gas and argon as collision gas. The capillary voltage was 3500 V, the source temperature was 150°C and the desolvation temperature was 350°C. Cone gas flow 50 L/h and desolvation gas 650 L/h. LPC(14:1) was measured in multiple reaction mode (MRM 466.3 > 104.1, cone 20 V, collision energy 23 V) and processed using Masslynx V4.2 (Waters). The peak area was normalized to the intensity of the internal standard D4-LPC(26:0) (MRM 640.5 > 104.1, cone 20 V, collision energy 30 V).

2.5 | Fragmentation analysis

Tandem mass spectrometry analysis (MS/MS) of the, at first instance unknown, lipid class was done using similar liquid chromatography mass spectrometry (LCMS) settings as described in the UPLC–HRMS section. MS/MS spectra were acquired in positive ion mode using higher

energy collisional dissociation (HCD) using a normalized collision energy of 10, 35, and 60 eV for the m/z corresponding to the unknown lipid class. MS/MS spectra were evaluated using Thermo Scientific Xcalibur 4.1.50.

2.6 | Annotation and statistical analyses

Peak identification in the untargeted lipidomics data was performed using a dedicated annotation tool written in MATLAB (<https://www.mathworks.com>), in which clusters of monoisotopic and labeled D9-lipid peaks could be annotated in a semi-automated fashion. Specifically, the identification of known lipids was based on a combination of accurate mass and an in-house database of retention times from earlier studies and relevant standards. Identification of unknown lipid clusters was based on the visualization of all unannotated peaks with significant patient-control group differences and the subsequent comparison of within cluster mass differences with a pre-established list of commonly occurring mass differences that was composed of naturally occurring isotopes (e.g. ^{13}C vs ^{12}C), chemical moieties (e.g. CH_2 , H_2 , O) and adducts (e.g. $[\text{M} + \text{H}]^+$ vs. $[\text{M} + \text{NH}_4]^+$).

Additional statistical analyses were performed using IBM SPSS Statistics for Windows, Version 26.0.0.1, Armonk, NY, IBM Corporation. Statistical significance of median differences between groups were calculated using a two-tailed Mann–Whitney U test. Correlation between to continuous variables was investigated using a Spearman's rank correlation test. p values below .05 were considered statistically significant. Data are presented as median with range.

3 | RESULTS

3.1 | Acylcarnitine accumulation patterns reflect lcFAOD enzyme deficiencies

Acylcarnitine levels in blood/plasma are generally thought to reflect intracellular levels of the corresponding acyl-CoA species. In line with this assumption, and with routine diagnostic procedures, we observed an increased relative abundance of disease-specific long-chain acylcarnitines (i.e., C18:1-carnitine in CPT2D, OH-C16:0-carnitine in LCHADD and MTPD, and C14:1-carnitine in VLCADD; Figure 1A) in lcFAOD patient fibroblasts cultured in standard HAM F-10 medium. When incubated with a medium containing deuterium-labeled oleic acid (D9-C18:1), we observed an increased relative abundance

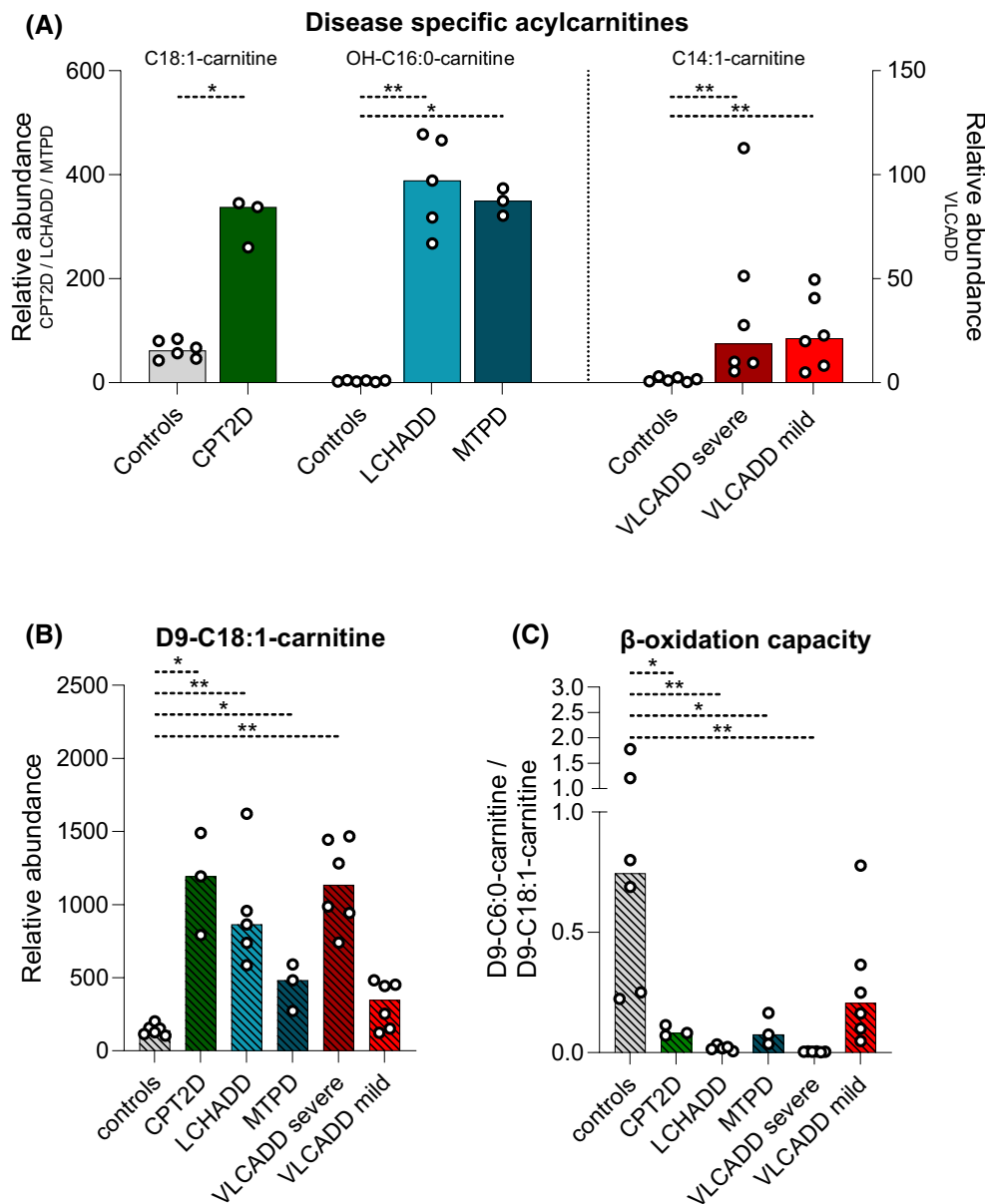


FIGURE 1 Disease-specific accumulation of acylcarnitines. (A) The disease-specific accumulation of long-chain acylcarnitines in CPT2D (C18:1-carnitine), LCHADD and MTPD (OH-C16:0-carnitine), and VLCADD (C14:1-carnitine) fibroblasts and control fibroblasts under standard culture conditions. (B) Increased relative abundance of D9-C18:1-carnitine 96 h after addition of D9-C18:1 to the medium as a consequence of the impaired β -oxidation in all lcFAOD fibroblasts compared to controls. (C) The ratio of D9-C6:0-carnitine (represents the product of β -oxidation) over D9-C18:1-carnitine (represents the substrate of β -oxidation) as a measure of the remaining flux of D9-C18:1 through the β -oxidation system. * $p < .05$; ** $p < .01$. Median (bars) and individual values (black circles) are shown in the graphs.

of D9-C18:1-carnitine, a derivative of the supplemented D9-C18:1 fatty acid, in all lcFAOD patients compared to control fibroblasts (Figure 1B) together with a decreased relative abundance of shorter intermediates in LCHADD and severe VLCADD patients (D9-C6:0- to D9-C10:0-carnitines; Figure 2A), indicating decreased β -oxidation capacity. Both the increased levels of disease-specific long-chain acylcarnitines and D9-C18:1-carnitine, and the decreased levels of short-chain D9-acylcarnitines

are in line with the lcFAO enzyme deficiency in patient fibroblasts.

For the here reported lcFAOD, the mitochondrial lcFAO capacity can be represented as the ratio of D9-C6-carnitine over D9-C18:1-carnitine, the product and the substrate, respectively. As expected, controls had the highest lcFAO capacity. In LCHADD and severe VLCADD lcFAO capacity was severely impaired, but in mild VLCADD, CPT2D and MPTD, there was residual lcFAO capacity (Figure 1C). For

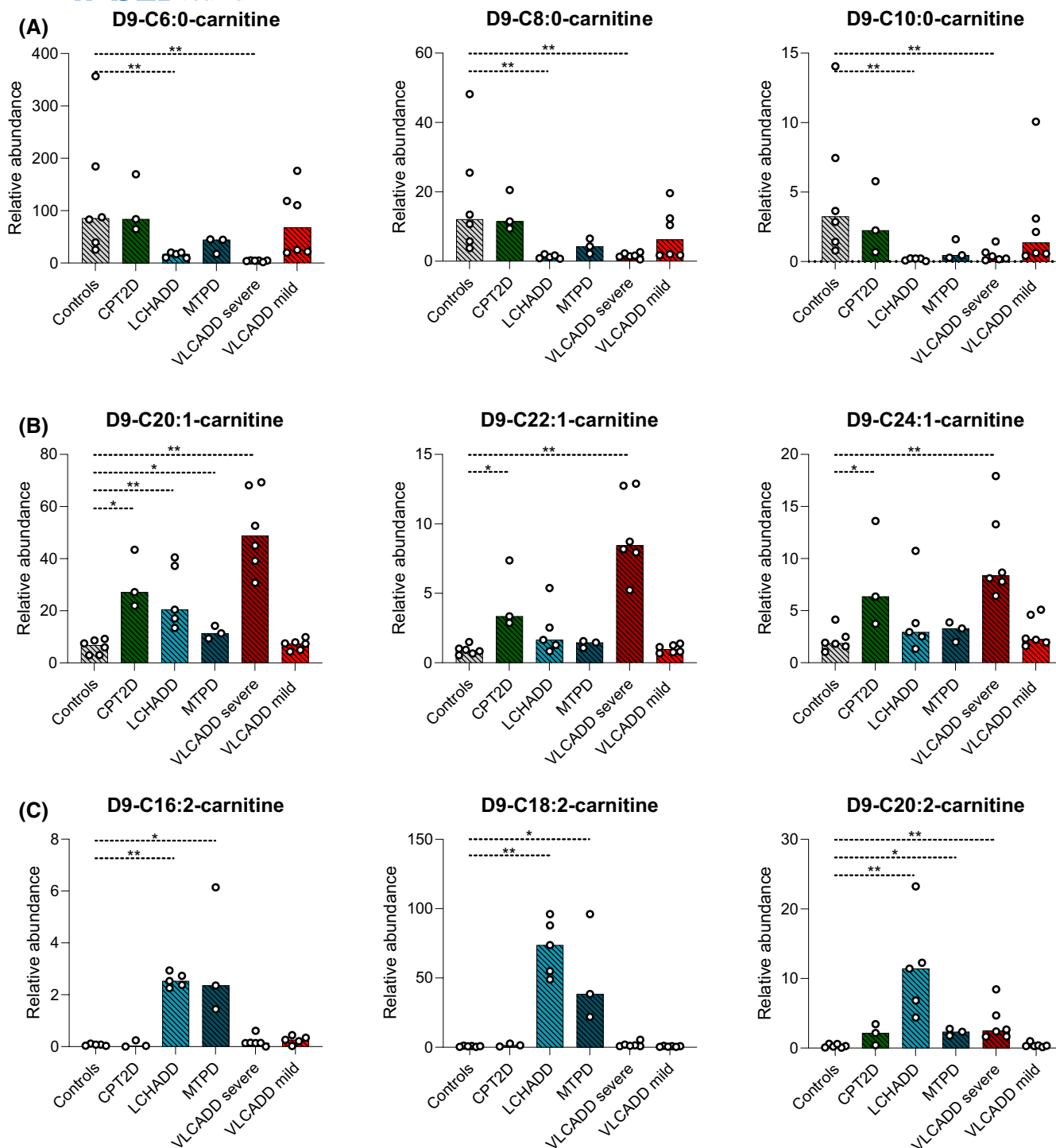


FIGURE 2 LcFAOD-specific handling of accumulating acylcarnitines. (A) Relative abundance of shorter chain acylcarnitines (D9-C6:0- to D9-C10:0-carnitine) in LcFAOD patient compared to control fibroblasts after addition of D9-C18:1 to the medium. (B) Relative abundance of long-chain (>C18) acylcarnitines in LcFAOD patient fibroblasts compared to control fibroblasts after addition of D9-C18:1 to the medium. (C) Relative abundance of unsaturated and long-chain (>C18) D9-acylcarnitines in LcFAOD patient compared to control fibroblasts after addition of D9-C18:1 to the medium. * $p < .05$; ** $p < .01$. Median (bars) and individual values (black circles) are shown in the graphs.

VLCADD, this ratio correlated well with the LcFAO flux as measured with tritium-labeled oleic acid, a validated diagnostic tool to measure the flux of oleic acid through the β -oxidation system and a good predictor of the VLCADD phenotype⁸ (Spearman's $\rho = 0.85$, $p < .001$, Figure S1A).

3.2 | Disease-specific lipid metabolism as identified by tracer-based lipidomics

When incubating CPT2D and VLCADD patient fibroblasts with D9-C18:1, we observed an increased relative

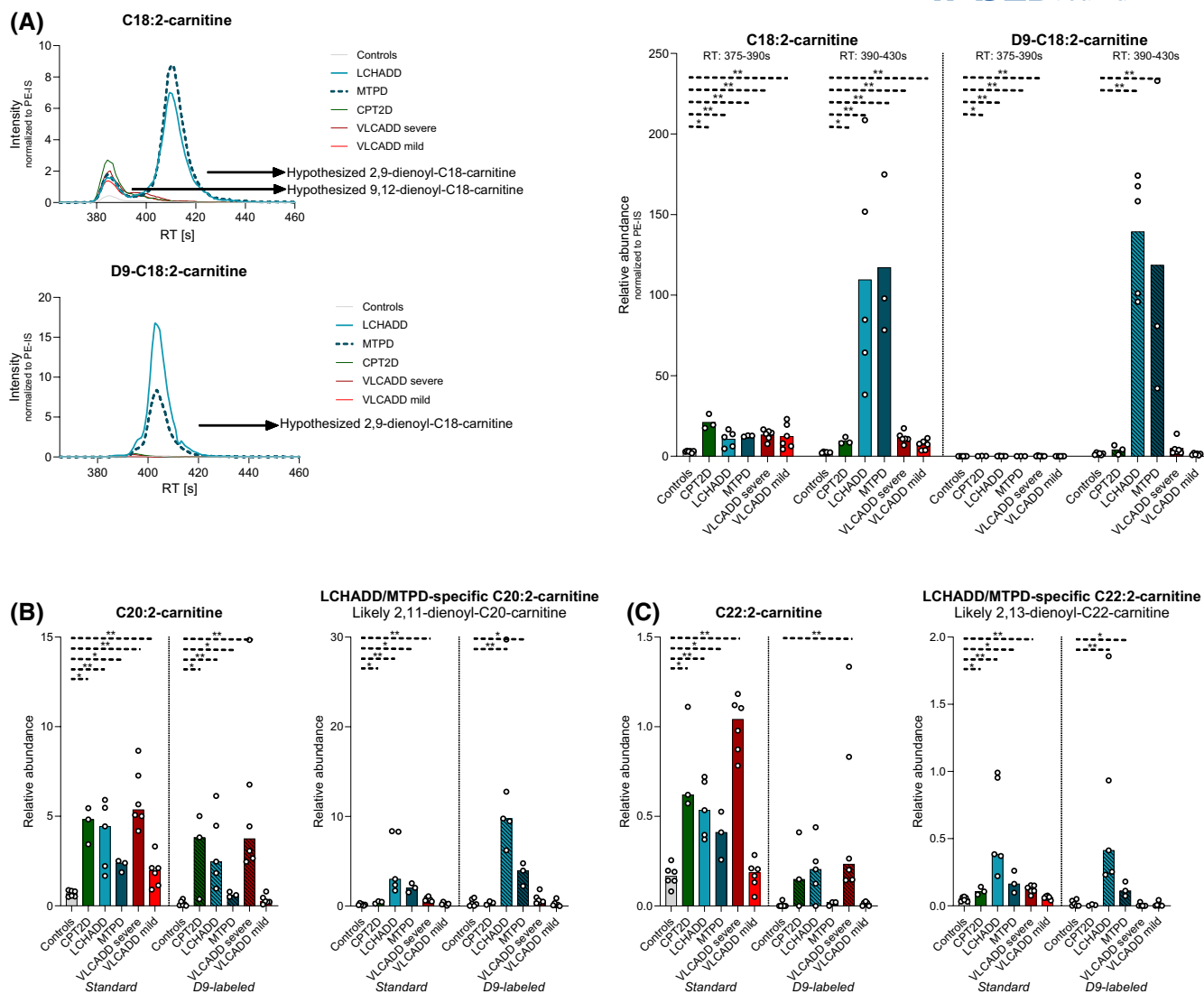


FIGURE 3 Disease-specific lipid metabolism leading to LCHADD and MTPD-specific acylcarnitines. (A) Extracted-ion chromatogram (left) and the relative abundance (normalized based on the PE internal standard) (right) of the two peaks of C18:2-carnitines measured with reverse phase liquid chromatography in control and lcFAOD patient fibroblasts cultured in standard conditions and after addition of D9-C18:1 to the medium. For the different acylcarnitine species, the peaks of the D9-labeled acylcarnitines had a slightly lower retention time (RT), likely as a consequence of the nine deuterium atoms that are heavier than their nonlabeled counterparts. Relative abundances of (D9-) C20:2-carnitine (B) and (D9-) C22:2-carnitine (C) and the LCHADD/MTPD-specific peaks, expected (D9-) 2,11-dienoyl-C20 (B), and (D9-) 2,13-dienoyl-C22-carnitines (C) measured with reverse phase liquid chromatography in control and lcFAOD patient fibroblasts cultured in standard conditions and after addition of D9-C18:1 to the medium. * $p < .05$; ** $p < .01$. Median (bars) and individual values (black circles) are shown in the graphs.

abundance of (very) long-chain, mono-unsaturated acylcarnitines (D9-C20:1-carnitines and longer) compared to controls, indicating elongation of D9-C18:1 (Figure 2B). In LCHADD and MTPD, lipidomics analysis using normal phase liquid chromatography identified an increase of long-chain acylcarnitines with two double bonds, namely of D9-18:2-carnitine, D9-20:2-carnitine, and, with a lower relative abundance, D9-C16:2-carnitine (Figure 2C). We detected two separate peaks in the extracted-ion chromatograms of C18:2-carnitine and D9-C18:2-carnitine (Figure 3A,B). The first eluting

peak (retention time (RT): 375–390s) was present in all lcFAOD, whereas the later eluting peak (RT: 390–430s) was only found in LCHADD and MTPD patient fibroblasts. This was also seen for C20:2-carnitine and C22:2-carnitine, although the relative abundances were increasingly lower (Figure 3C). We speculate that these LCHADD- and MTPD-specific lipid acylcarnitine species are carnitine esters that originate from the VLCAD-dependent dehydrogenation of D9-9-enoyl-C18-CoA (D9-)oleyl-carnitine and its elongation products D9-11-enoyl-C20-CoA and D9-13-enoyl-C22-CoA, resulting

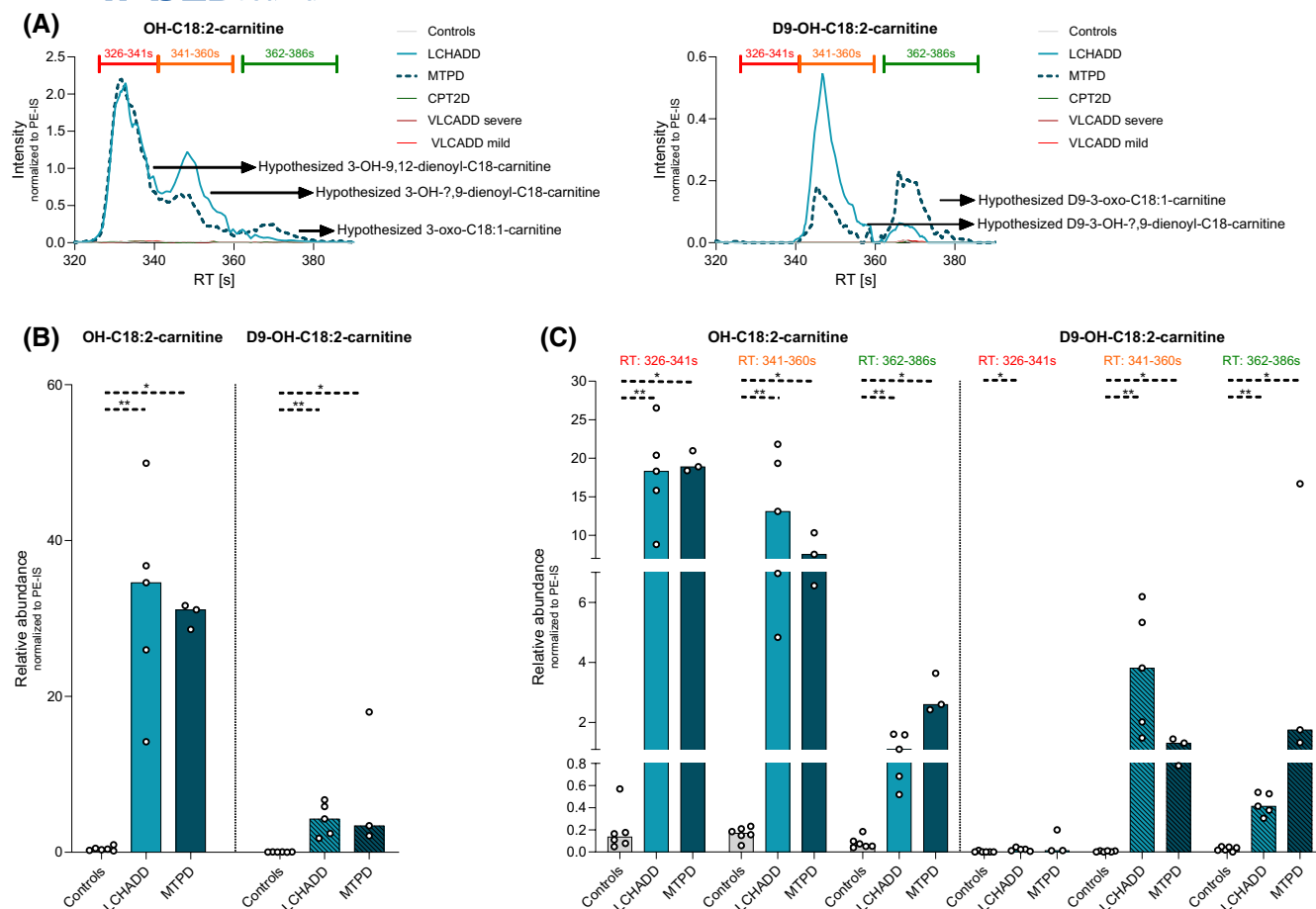


FIGURE 4 LCHADD and MTPD-specific accumulation of hydroxyacylcarnitine species. (A) Extracted-ion chromatogram of OH-C18:2-carnitine (left) and D9-OH-C18:2-carnitine (right). For the OH-C18:2-carnitine, we observed three peaks. The peaks were hypothesized to be 3-OH-9,12-dienoyl-C18-carnitine (first peak, retention time (RT): 326–341 s, red), 3-OH-7,9-dienoyl-C18-carnitine (second peak, RT: 341–360 s, orange, position double bond unknown) and 3-oxo-C18:1-carnitine (third peak, RT: 362–386 s, green). For the labeled analysis, D9-OH-C18:2-carnitine, we only observe two peaks, hypothesized to be D9-3-OH-7,9-dienoyl-C18-carnitine (first peak) and, D9-3-oxo-C18:1-carnitine (second peak). (B) Relative abundance of OH-C18:2-carnitine and D9-OH-C18:2-carnitine in LCHADD and MTPD patients compared to controls. (C) Relative abundance of OH-C18:2-carnitine and D9-OH-C18:2-carnitine for the different peaks (based on RT) observed in A. * $p < .05$; ** $p < .01$. Median (bars) and individual values (black circles) are shown in the graphs.

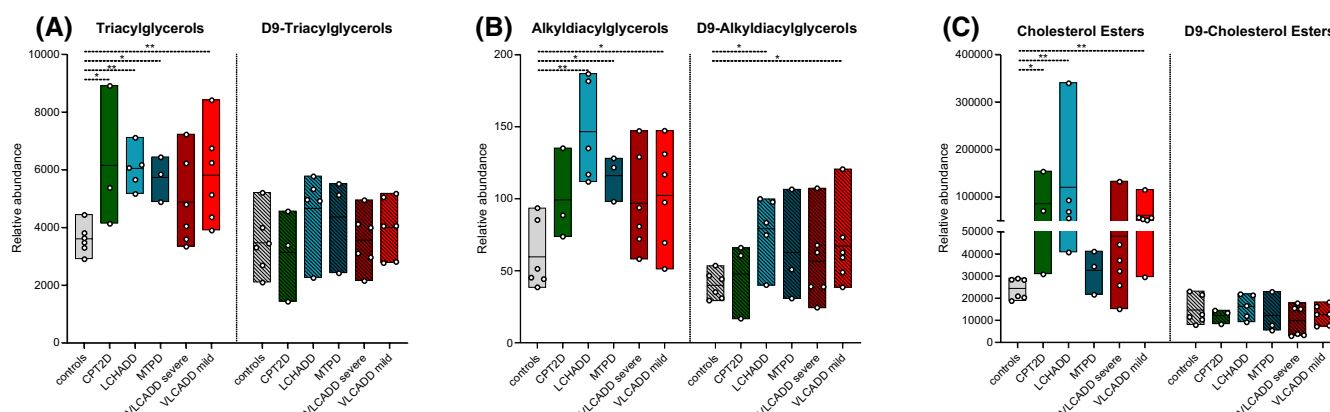


FIGURE 5 Neutral lipids accumulate in lFAOD fibroblasts. The relative abundance of neutral lipids (TG, TG(O), and CE) in lFAOD patient fibroblasts compared to control fibroblasts cultured in standard conditions and after addition of D9-C18:1 to the medium. * $p < .05$; ** $p < .01$. Median (black lines) and individual values (open circles) are shown in the graphs. The boxes span the minimal and maximal observed value.

in the respective formation of D9-2,9-dienoyl-C18-CoA (D9-C18:2-CoA), D9-2,11-dienoyl-C20-CoA (=D9-C20:2-CoA) and D9-2,13-dienoyl-C22-CoA (=D9-C22:2-CoA) (Figure S2A). We observed a negative correlation between the calculated mitochondrial lcFAO capacity and the levels of D9-2,11-dienoyl-C20-carnitine accumulation in LCHADD and MTPD (Spearman's $\rho = -0.86$, $p = .01$, Figure S1B). This negative correlation indicated that more D9-9-enoyl-C18-CoA is elongated and consequently more D9-2,11-dienoyl-C20-carnitine is formed in case of a lower mitochondrial lcFAO capacity caused by a more severe downstream metabolic block.

These results were confirmed in patient fibroblasts cultured in standard medium, where we also observed increased levels of very long-chain acylcarnitines (>C22) in VLCADD compared to controls, and increased levels of double unsaturated acylcarnitines in LCHADD and MTPD compared to controls and other lcFAOD patient fibroblasts (Figure S3).

3.3 | LCHADD and MTPD cells accumulate specific hydroxyacylcarnitine species

To investigate possible differences in the LCHADD- and MTPD-specific OH-C18:1- and OH-C18:2-carnitine species we evaluated their extracted-ion chromatograms derived from the reversed-phase analysis. For both OH-C18:1-carnitine and D9-OH-C18:1-carnitine, we detected one peak (RT: 366–398s), likely corresponding to the 3-hydroxyl form of (D9-)oleoyl-carnitine (Figure S4). However, for OH-C18:2-carnitine, we detected three peaks (Figure 4). Like for (D9-)9-enoyl-C18-carnitine, (D9-)11-enoyl-C20-carnitine and (D9-)13-enoyl-C22-carnitine, the peaks of the labeled substrates were shifted to slightly lower retention times compared to the unlabeled substrates. We hypothesize that the first eluting peak (RT: 326–341 s) corresponds to the 3-hydroxyl form of linoleoyl-carnitine (3-OH-9,12-dienoyl-C18-carnitine). The second and third eluting peaks (RT 341–360s and 362–386s, respectively) were also found in the extracted-ion chromatogram of D9-labeled OH-C18:2-carnitine, indicating that both peaks were products of the added D9-C18:1. The second eluting peak was predominantly present in LCHADD- and to a lesser extent in MTPD-patient fibroblasts when compared to controls. We hypothesized that the second peak at RT 341–360s was a product of fatty acid desaturases (FADS)^{21,22} forming D9-?,9-dienoyl-C18-CoA (“?” represents the unknown location of the new double bond) followed by partial oxidation through the lcFAO pathway to form D9-?,9-dienoyl-3-OH-C18-CoA and its corresponding acylcarnitine, see discussion (Figure S2B). The

third, MTPD-specific, peak at RT 362–386s is most likely (D9-)3-oxo-C18:1-carnitine, the intermediate accumulating due to a deficiency of the LCKAT activity (Figure S2B).

3.4 | Neutral lipid accumulation in lcFAOD fibroblasts

In lcFAOD patient fibroblasts cultured in standard medium we observed neutral lipid accumulation. The median sums of all triacylglycerols (TG), alkyl diacylglycerols (TG(O)) and cholesterol esters (CE) were significantly higher in lcFAOD compared to control fibroblasts (1.6, 2.4 and 2.1 times, respectively). There were however differences between the distinct lcFAOD: TG(O) and CE were increased in LCHADD, and not or only mildly in other lcFAOD (Figure 5A,B). CE levels were normal in severe VLCADD and MTPD (Figure 5C). The group of mild VLCADD patients with high lcFAO fluxes (33%–125%), but not the severe VLCADD patients with low lcFAO fluxes (5%–7%), showed neutral lipid accumulation (Table 1, Figure 5). There was no statistically significant correlation between the amount of lipid accumulation (TG, TG(O) and CE) and lcFAO flux in VLCADD patients (not shown).

After D9-C18:1 loading to allow lipid tracing, the relative abundance of TG(O) was significantly increased in LCHADD and mild VLCADD, whereas D9-neutral lipids were not increased in other lcFAOD patient fibroblasts when compared to controls (Figure 5). Comparison of chain-length distribution and saturation patterns in neutral lipid chains with disease-specific acylcarnitine patterns did not show consistent effects (Table S1). The relative abundance of phospholipids (phosphatidylcholine (PC), phosphatidylethanolamine (PE)) and lysophospholipids (lysophosphatidylcholine (LPC) and lysophosphatidylethanolamine (LPE)) was normal or slightly decreased compared to controls with and without D9-C18:1 added to the medium (Figure S5). The ratio of PC and PE was comparable to the levels of the controls under both conditions (Table S1). In conclusion, we observed a neutral lipid accumulation (TG, TG(O) and CE) in lcFAOD patient fibroblasts cultured in standard medium, albeit the accumulation varied between the different disorders. (Lyso)phospholipids, on the other hand, were not clearly affected at the class level.

3.5 | LPC(14:1) is a VLCADD-specific candidate biomarker that correlates with VLCAD enzyme activity

Although lysophospholipids as a group were not increased in lcFAOD patients, LPC(14:1) was significantly

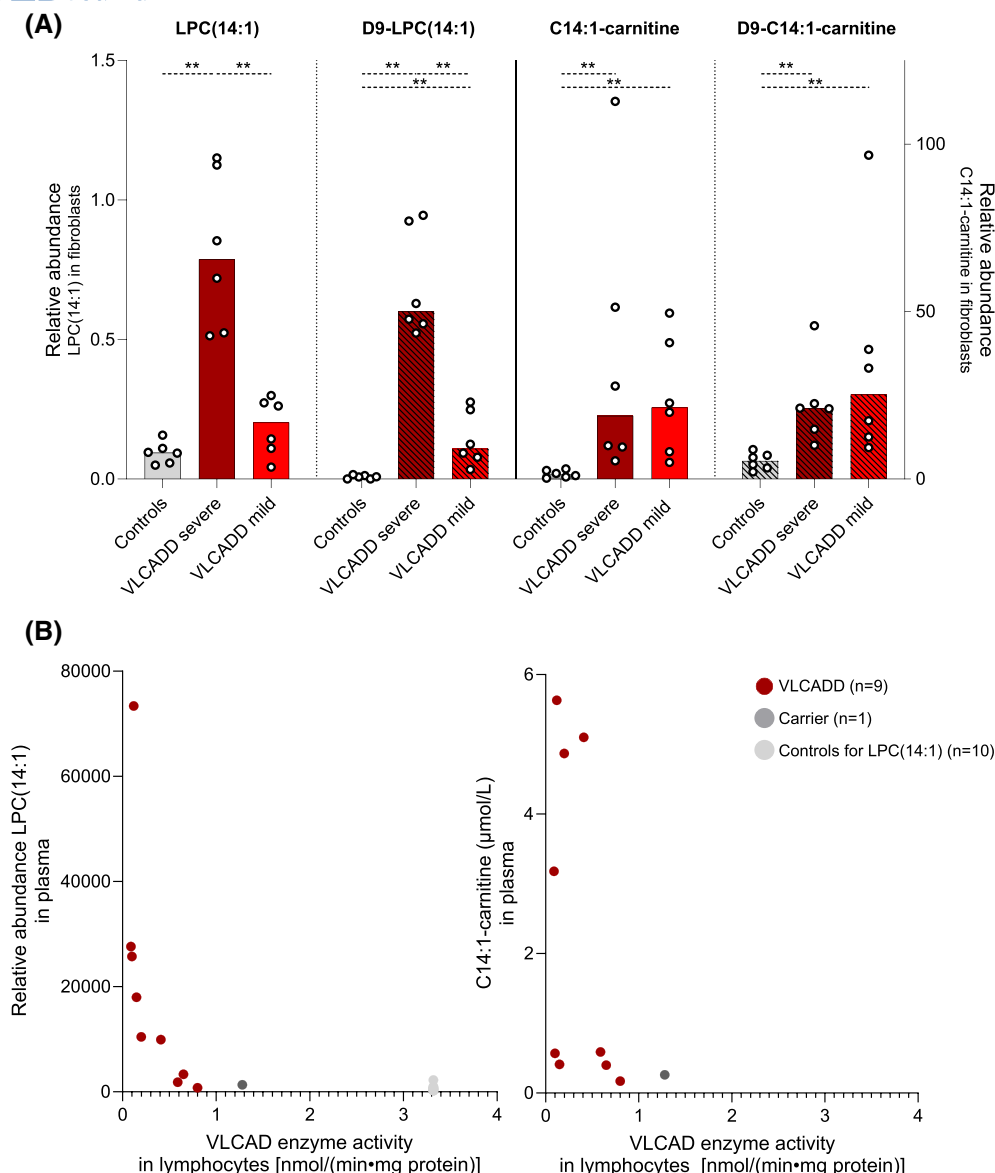


FIGURE 6 LPC(14:1) as new VLCADD disease severity marker. (A) Relative abundance of LPC(14:1) and D9-LPC(14:1) in mild and severe VLCADD patient fibroblasts and control fibroblasts cultured in standard conditions and after addition of D9-C18:1 to the medium. * $p < .05$. ** $p < .01$. Median (bars) and individual values (open circles) are shown. (B) LPC(14:1) and C14:1-carnitine were measured in plasma samples from VLCADD patients with varying remaining enzyme activities ($n = 9$) (red dots), a carrier of a variant in *ACADVL* ($n = 1$) (dark gray dot), and, for LPC(14:1), healthy controls ($n = 10$) (light gray dots).

more abundant in severe VLCADD patient fibroblasts compared to controls (Figure 6A). This lipid better discriminated between mild and severe VLCADD than the established VLCADD biomarker C14:1-carnitine and had a higher correlation with lcFAO flux (Spearman's ρ lcFAO flux and LPC(14:1): -0.82 , $p = .001$, Spearman's ρ lcFAO flux and C14:1-carnitine: -0.13 , $p = .70$). Similarly, D9-LPC(14:1) had a significantly higher abundance in severe VLCADD compared to mild VLCADD and control fibroblasts (Figure 6A). To further investigate LPC(14:1) as a possible VLCADD disease severity marker, we measured LPC(14:1) in plasma of ten healthy controls, one carrier of VLCADD, and nine VLCADD patients with varying

clinical and biochemical phenotypes (Table S2). LPC(14:1) accumulation in plasma of VLCADD patients showed a strong correlation with enzyme activity measured in lymphocytes (Spearman's $\rho = -0.93$, $p < .001$) (Figure 6B). The correlation of LPC(14:1) with enzyme activity was better than the correlation of C14:1-carnitine with enzyme activity (Spearman's ρ enzyme activity and C14:1-carnitine: -0.48 , $p = .19$, respectively (Figure 6B)). Correlating LPC(14:1) concentrations with the clinical phenotype was complicated by the relatively low number of patients and the fact that this cohort contains both symptomatically- and NBS-diagnosed patients with varying follow-up times. Nevertheless, LPC(14:1) was increased in all symptomatic

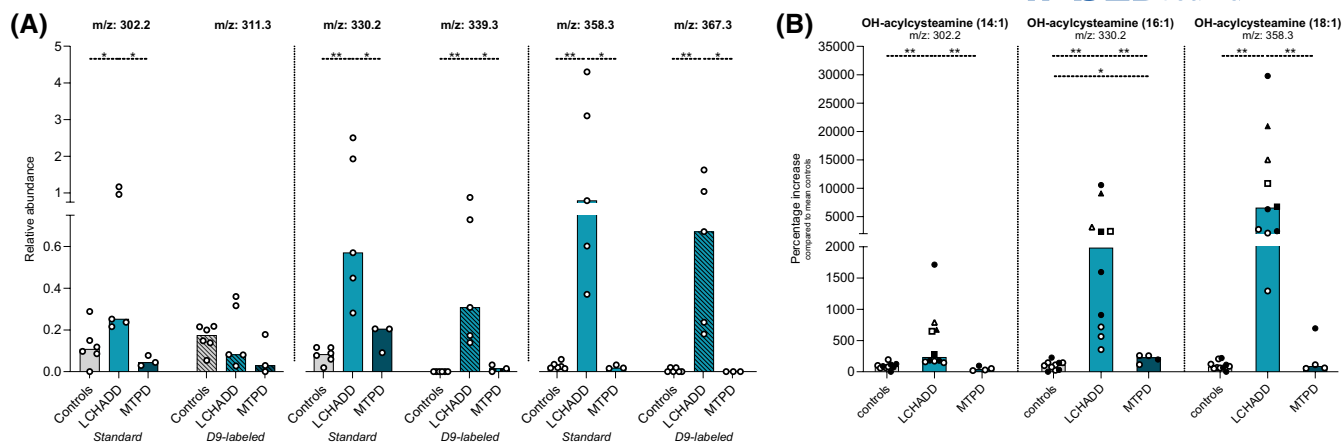


FIGURE 7 S-(3-hydroxyacyl)cysteamines are new disease markers for LCHADD. (A) Endogenous and corresponding D9-C18:1-derived features, likely S-(3-hydroxyacyl)cysteamines, were detected in significantly higher abundance in LCHADD patient fibroblasts when compared to control and MTPD patient fibroblasts cultured in standard conditions and after addition of D9-C18:1 to the medium. (B) Lipidomics analysis in fibroblast pellets from LCHADD patients ($n=5$) (two cell lines were also included in the original lipidomics experiment: LCHADD_3 and LCHADD_4, Table S3), an MTPD patient ($n=1$) and controls ($n=4$). Graphs show the combined results of the first (open circles) and the second (closed circles) lipidomics analysis. $*p < .05$; $**p < .01$. Median (bars) and individual values (circles) are shown as percentage of the controls' average in the same experiment. LCHADD_3 and LCHADD_4 were also measured in the repeat experiment (analysis of new/unrelated sample) and are shown in triangle and square symbols, respectively.

patients and one asymptomatic NBS-diagnosed patient with a low lcFAO flux ($\leq 10\%$) associated with a severe clinical phenotype, whereas LPC(14:1) was normal compared to controls in one asymptomatic NBS-diagnosed patient with a high lcFAO flux (not shown).

3.6 | S-(3-hydroxyacyl)cysteamines are LCHADD-specific candidate biomarkers

Using untargeted lipidomics, which allowed detection of ~40 000 features, we identified a set of unknown features that were significantly elevated only in LCHADD when compared to controls and other lcFAOD patient fibroblasts (Figure 7A). The m/z values of the unknown features differed from each other by the mass of two methylene groups. After incubation with D9-C18:1, the D9-tracer was also incorporated in these, at that time unknown, features indicating that they are part of a lipid cluster containing fatty acids or their derivatives. Interestingly, in MTPD patient fibroblasts, this newly identified lipid cluster was not significantly increased. Fragmentation analysis was in line with the hypothesis that this unknown lipid cluster likely corresponded to thioesters of cysteamine, possibly originating from the degraded Coenzyme A-moiety, and a hydroxy-fatty acid (with varying chain lengths) (Figure S6). We termed these molecules S-(3-hydroxyacyl)cysteamines.

To confirm our findings, we repeated the lipidomics analysis in anonymized dermal fibroblast pellets not controlled for culture conditions and storage duration,

from four healthy controls, one MTPD patient, and five LCHADD patients, again showing a significant increase in the LCHADD samples (Figure 7B). To exclude that the S-(3-hydroxyacyl)cysteamines were artifacts produced during sample preparation, we determined the concentration dependency of D9-C18:1-OH-cysteamine formation from D9-C18:1 in fibroblasts of one control and one LCHADD patient. For the highest D9-C18:1 concentration we also directly lysed cells in methanol:chloroform to exclude non-enzymatic formation of S-(3-hydroxyacyl)cysteamines. Strikingly, D9-C18:1-OH-cysteamine was formed in a D9-C18:1-concentration-dependent manner and was also present in the directly lysed cells, confirming that S-(3-hydroxyacyl)cysteamines are endogenously produced metabolites (Figure S7).

4 | DISCUSSION

Since the discovery of the first lcFAOD patients around the 1980s, diagnostic and therapeutic strategies have improved significantly, including implementation of lcFAOD in NBS programs allowing for pre-symptomatic diagnosis and treatment from birth. This has not only helped to prevent life-threatening hypoglycemia, but with time also showed that there still are difficulties to predict prognosis pre-symptomatically. Moreover, treatment strategies for some disorders are limited. Better understanding of the metabolic consequences of lcFAOD will likely contribute to further improving care for these patients. In this study we used tracer-based lipidomics in

CPT2D, LCHADD, MTPD and VLCADD patient fibroblasts to investigate the fate of LCFAs in lcFAOD, and the potential role of accumulating lcFAO intermediates in lcFAOD pathophysiology.

We observed a direct correlation between the chain length and saturation patterns of accumulating acylcarnitines with the enzyme deficiencies in lcFAOD. For CPT2D and VLCADD, we mainly detected accumulation of elongated mono-unsaturated acylcarnitines, whereas for LCHADD and MTPD, acylcarnitines with an additional double bond accumulated. We hypothesized that these LCHADD- and MTPD-specific lipid acylcarnitine species are carnitine esters that originate from VLCAD-dependent dehydrogenation of long-chain acyl-CoAs, yielding 2-enoyl-acyl-CoAs. Based on the combination of (1) the accumulation of both elongated mono-unsaturated (for CPT2D and VLCADD) and the presumed 2-enoyl-acylcarnitines (for LCHADD and MTPD), (2) the low affinity of CPT2 for 2-enoyl-acyl-CoAs,²³ which makes the transport of 2-enoyl-acyl-CoAs out of the mitochondria unlikely, (3) the fact that enzymes catalyzing the elongation of fatty acids are present outside of the mitochondria (mainly the endoplasmic reticulum²⁴) and (4) elongation enzymes present within the mitochondria mainly act on substrates shorter than 16 atoms,²⁵ we suggest that accumulating fatty acids (e.g., C18:1) are first transported out of mitochondria (via the carnitine cycle), then elongated in the endoplasmic reticulum (e.g., to C20:1), subsequently transported back into mitochondria followed by dehydrogenation by VLCAD (e.g., to form C20:2).

By tracer-based lipidomics and analysis of extracted-ion chromatograms of selected acylcarnitines, we found that there was alternative and disease-specific processing of accumulating lcFAO-intermediates. This is concluded from the finding of different chromatographic peaks in the extracted-ion chromatograms corresponding to different species of (D9-)OH-C18:2-carnitine in LCHADD and MTPD. Based on the stable isotope labeling experiment, we reasoned that the first and the third peak corresponded to the 3-hydroxyl form of linoleoyl-carnitine (3-OH-9,12-dienoyl-C18-carnitine) and 3-oxo-9-enoyl-C18 carnitine, respectively. The second peak, however, was only present in the labeling experiment and thus must have been derived from the D9-C18:1 which had gained an hydroxyl-group and an additional double bond to form (D9-)OH-C18:2, most likely introduced by the “general” desaturase FADS2.^{21,22} We hypothesize that the (D9-)C18:1-CoA which now contains a second double bond introduced by the FADS enzyme (i.e. (D9-)9-enoyl-C18-CoA to produce (D9-)C18:2-CoAs (position of double bond unknown)), is subsequently imported into mitochondria to be degraded via β -oxidation. Given the impairment

in lcFAO because of LCHADD, β -oxidation is disturbed and (D9-)3-OH-C18:2-carnitine accumulates. These different species of OH-C18:2-carnitines illustrate the complex metabolic consequences of lcFAOD and highlight the insight that labeling studies in combination with UPLC-MS can yield.

Based on previous findings of neutral lipid accumulation due to impaired lcFAO both in vitro and in vivo,^{10–13,15,26} we hypothesized that disease-specific lcFAO-intermediates are shunted towards neutral lipid species such as TG as a protection mechanism. Indeed, we observed neutral lipid accumulation (TG, TG(O) and CE) in lcFAOD fibroblasts cultured in standard medium. (Lyso)phospholipids, however, did not accumulate, and in some lcFAOD the levels of these lipid species were even decreased. Moreover, we observed no changes in the PC/PE ratio, which was previously associated with mitochondrial disease^{27–29} and LCHADD.¹⁵ The observed changes in neutral lipids but not in (lyso)phospholipids may relate to the different functions of these lipid species and likely are tissue/cell type specific. Whereas neutral lipids mainly function as energy storage, (lyso)phospholipids are essential signaling molecules^{30,31} and building blocks for cellular and organellar membranes.³² To prevent large changes in these structural/functional lipids, cells may shunt accumulating fatty acids into “storage” lipids as exemplified by steatosis of liver and muscle in lcFAOD.^{33–35} However, tracing of D9-C18:1 did not provide direct evidence for storage of LCFAs in neutral lipids in lcFAOD fibroblasts. Supplementation of carnitine to the culture medium together with the D9-C18:1 may have stimulated detoxification through acylcarnitine formation and excretion in the medium. Also, the time-scale of the experiment could have been too short to accumulate D9-labeled fatty acids in neutral lipids.

C14:1-carnitine, the (NBS) marker for VLCADD, accumulated similarly in both severe and mild VLCADD patient fibroblasts. lcFAO flux measurements can discriminate between mild and severe VLCADD phenotypes,⁸ but obtaining dermal fibroblasts for this is both invasive and time-consuming with limited test accessibility. We here found that LPC(14:1) also differentiated between severe and mild VLCADD in fibroblasts. Furthermore, we observed a correlation between LPC(14:1) in plasma from VLCADD patients and enzyme activity. Although promising, this initial observation does require confirmation in more patients and further characterization in terms of reproducibility, accuracy, specificity and sensitivity, before a potential implementation in clinical practice.

LPCs are the most abundant lysoglycerophospholipids in human blood, and are suggested to play, among other functions, a role in the inflammatory response with both pro- and anti-inflammatory effects.^{36–38} LPCs can

become toxic to cells at high concentrations, as they disrupt membrane structures and cause cell lysis, hence the prefix “lyso”. LPCs are derived from the corresponding phospholipid PC via hydrolysis by lipoprotein-associated phospholipases A₁ or A₂.³⁸ Long-chain LPCs are used as biomarkers for other metabolic diseases. For example, LPC(26:0) is used as a biomarker of very LCFA accumulation in adrenoleukodystrophy (ALD) and can be detected in blood spots.³⁹ In VLCADD, accumulating C14:1 is likely integrated into PC eventually leading to the formation of LPC(14:1). As a product of PC, LPCs may be more stable and have a longer half-life in plasma than acylcarnitines, which are highly influenced by the patient's diet, fasting and exercise.⁴⁰ If LPCs have a longer half-life, they might better represent the accumulating β -oxidation intermediates over a longer time period which is less influenced by the exact sampling time. Although possible dietary and lifestyle influences on LPC(14:1) still need to be investigated, plasma LPC(14:1) may thus represent a useful candidate biomarker to predict disease severity and monitor the effects of and compliance to dietary interventions.

Using untargeted lipidomics, we discovered a potential LCHADD-specific candidate biomarker, which accumulated specifically in LCHADD patient fibroblasts in two separate experiments, including cell pellets of fibroblasts cultured under different conditions and at different time points. Based on the *m/z* values, fragmentation analysis, and the presence of a cluster of lipids with a fatty acid signature, we provisionally identified these lipids as S-(3-hydroxyacyl)cysteamines. We hypothesize that the generation of S-(3-hydroxyacyl)cysteamines occurs due to the high concentrations of 3-hydroxyacyl-CoAs that accumulate in LCHADD caused by the β -oxidation defect in combination with putatively lower affinity towards conversion into acylcarnitines (via CPT2) and cleavage into free fatty acids and coenzyme A (via thioesterases).²³ The accumulating 3-hydroxyacyl-CoAs may be shunted into the CoA degradation pathway leading to the formation of S-(3-hydroxyacyl)cysteamines.^{41,42} The exact mechanism of the generation of these lipid species is as yet unknown and requires further investigation. However, two enzymatic pathways/enzymes exist which in theory could produce S-(3-hydroxyacyl)cysteamines, pantheteinase (VNN)⁴² and/or amidase^{43,44} activity. Pantheteinase catalyzes the last step of the CoA degradation pathway, but is generally regarded as an extracellular protein⁴² making this possibility less likely. Accumulating 3-hydroxyacyl-CoAs could also be processed by an amidase, an enzyme that previously has been described to catalyze the one-step generation of acylcysteamines from acyl-CoAs.^{43,44}

We observed that S-(3-hydroxyacyl)cysteamines almost exclusively accumulated in LCHADD fibroblasts, whereas only minimal or inconsistent accumulation

was observed in MTPD. Most of our MTPD patients had mild disease with relatively high residual enzyme activity and lcFAO capacity, likely allowing some degradation of 3-hydroxyacyl-CoAs via the β -oxidation pathway. Yet, it remains puzzling that hydroxyacylcarnitines accumulated in both LCHADD and MTPD, suggesting that hydroxyacyl-CoAs do so too, and that concomitantly S-(3-hydroxyacyl)cysteamines would be expected to be formed in both disorders.

The LCHADD specificity of the S-(3-hydroxyacyl)cysteamines and the precise mechanism of formation still requires further investigation. However, our findings suggest that 3-hydroxyacyl-CoAs, and possibly also other accumulating acyl-CoAs, can be driven towards the CoA degradation pathway leading to the formation of S-(3-hydroxyacyl)cysteamines. LCHADD and MTPD are unique among lcFAOD as they are the only two lcFAOD that display pigmentary retinopathy and peripheral neuropathy. For long, it was thought that toxic effects of accumulating 3-hydroxyacyl-CoAs and their carnitine derivatives may play a role in the development of these long-term complications. The exact pathophysiological mechanism, however, remains unknown. Our discovery of the predominant and specific occurrence of S-(3-hydroxyacyl)cysteamines in LCHADD makes it tempting to speculate that they might play a role in LCHADD- (and MTPD-) specific disease pathophysiology. CoA biosynthesis deficiencies present with severe neurological phenotypes, including axonal neuropathy and pigmentary retinopathy due to CoA shortage.^{45–47} We hypothesize that activity of the CoA degradation pathway in LCHADD and possibly MTPD may also result in CoA shortage which in turn might contribute to the development of pigmentary retinopathy and peripheral neuropathy.

In conclusion, we observed neutral lipid without (lyso) phospholipid accumulation in lcFAOD fibroblasts, suggesting protection of the intracellular balance in functional lipids by shunting accumulating fatty acids into neutral lipids. Tracer-based lipidomics did not only increase insight in the (alternative) processing and fate of accumulating lcFAO-intermediates in lcFAOD, but also enabled the discovery of two disease-specific candidate biomarkers, LPC(14:1) for VLCADD and S-(3-hydroxyacyl)cysteamines for LCHADD, which may have significant relevance for disease prognosis and diagnosis, respectively.

AUTHOR CONTRIBUTIONS

Marit Schwantje, Signe Mosegaard, Riekelt H Houtkooper, Sacha Ferdinandusse, and Frédéric M. Vaz: conceptualization; Suzan J. G. Knottnerus, Frédéric M. Vaz, Henk van Lenthe, Jill Hermans, Simone W Denis, and Yorrick R. J. Jaspers: methodology; Jan Bert van Klinken, Marit Schwantje, and Signe Mosegaard: formal analysis; Marit

Schwantje, Signe Mosegaard, Suzan J. G. Knottnerus, Henk van Lenthe, Jill Hermans Simone W Denis, and Yorrick R. J. Jaspers: investigation; Marit Schwantje, Signe Mosegaard, Riekelt H. Houtkooper, Sacha Ferdinandusse, and Frédéric M. Vaz: writing – original draft; Marit Schwantje, Signe Mosegaard, Ronald J Wanders, Sabine A. Fuchs, Riekelt H. Houtkooper, Sacha Ferdinandusse, and Frédéric M. Vaz: writing – review & editing, Marit Schwantje, Signe Mosegaard, Frédéric M. Vaz: visualization.

FUNDING INFORMATION

MS was supported by Metakids and PNO Zorg (2019_087). SM was supported by an International Postdoc grant from Independent Research Fund Denmark (1057-00039B). Work in the Houtkooper lab is financially supported by a NWO Middelgroot grant (no. 91118006).

DISCLOSURES

The authors declare that they have no conflicts of interest related to this article.

DATA AVAILABILITY STATEMENT

Raw data included in the manuscript will be available upon reasonable request from the corresponding author.

ORCID

Marit Schwantje  <https://orcid.org/0000-0003-4775-1760>

Signe Mosegaard  <https://orcid.org/0000-0002-4561-1978>

Sabine A. Fuchs  <https://orcid.org/0000-0001-9147-2406>

Riekelt H. Houtkooper  <https://orcid.org/0000-0001-9961-0842>

Sacha Ferdinandusse  <https://orcid.org/0000-0002-7738-5709>

Frédéric M. Vaz  <https://orcid.org/0000-0002-9048-1041>

REFERENCES

- Houten SM, Violante S, Ventura FV, Wanders RJA. The biochemistry and physiology of mitochondrial fatty acid β -oxidation and its genetic disorders. *Annu Rev Physiol*. 2015;78:23-44. doi:10.1146/annurev-physiol-021115-105045
- Nielson JR, Rutter JP. Lipid-mediated signals that regulate mitochondrial biology. *J Biol Chem*. 2018;293:7517-7521.
- van Meer G, Voelker DR, Feigenson GW. Membrane lipids: where they are and how they behave. *Nat Rev Mol Cell Biol*. 2008;9:112-124.
- Knottnerus SJG, Bleeker JC, Wüst RCI, et al. Disorders of mitochondrial long-chain fatty acid oxidation and the carnitine shuttle. *Rev Endocr Metab Disord*. 2018;19:93-106.
- Das AM, Illsinger S, Lucke T, et al. Isolated mitochondrial long-chain ketoacyl-CoA Thiolase deficiency resulting from mutations in the HADHB gene. *Clin Chem*. 2006;52:530-534.
- Kruger E, McNiven P, Marsden D. Estimating the prevalence of rare diseases: long-chain fatty acid oxidation disorders as an illustrative example. *Adv Ther*. 2022;39:3361-3377.
- Marsden D, Bedrosian CL, Vockley J. Impact of newborn screening on the reported incidence and clinical outcomes associated with medium- and long-chain fatty acid oxidation disorders. *Genet Med*. 2021;23:816-829.
- Diekman EF, Ferdinandusse S, van der Pol L, et al. Fatty acid oxidation flux predicts the clinical severity of VLCAD deficiency. *Genet Med*. 2015;17:989-994.
- Knottnerus SJG, Mengarelli I, Wüst RCI, et al. Electrophysiological abnormalities in VLCAD deficient hiPSC-cardiomyocytes can be improved by lowering accumulation of fatty acid oxidation intermediates. *Int J Mol Sci*. 2020;21:2589.
- Laforêt P, Acquaviva-Bourdain C, Rigal O, et al. Diagnostic assessment and long-term follow-up of 13 patients with Very Long-Chain Acyl-Coenzyme A dehydrogenase (VLCAD) deficiency. *Neuromuscul Disord*. 2009;19:324-329.
- Laforêt P, Vianey-Saban C. Disorders of muscle lipid metabolism: diagnostic and therapeutic challenges. *Neuromuscul Disord*. 2010;20:693-700.
- Purevsuren J, Fukao T, Hasegawa Y, et al. Clinical and molecular aspects of Japanese patients with mitochondrial trifunctional protein deficiency. *Mol Genet Metab*. 2009;98:372-377.
- Shchelochkov O, Wong L-J, Shaibani A, Shinawi M. Atypical presentation of VLCAD deficiency associated with a novel ACADVL splicing mutation. *Muscle Nerve*. 2009;39:374-382.
- Polinati PP, Ilmarinen T, Trokovic R, et al. Patient-specific induced pluripotent stem cell-derived RPE cells: understanding the pathogenesis of retinopathy in long-chain 3-hydroxyacyl-CoA dehydrogenase deficiency. *Invest Ophthalmol Vis Sci*. 2015;56:3371-3382.
- Alatibi KI, Hagenbuchner J, Wehbe Z, et al. Different lipid signature in fibroblasts of long-chain fatty acid oxidation disorders. *Cell*. 2021;10:1239.
- Verkerk AO, Knottnerus SJG, Portero V, et al. Electrophysiological abnormalities in VLCAD deficient hiPSC-cardiomyocytes do not improve with carnitine supplementation. *Front Pharmacol*. 2021;11:616834.
- Smith PK, Krohn RI, Hermanson GT, et al. Measurement of protein using bicinchoninic acid. *Anal Biochem*. 1985;150:76-85.
- Molenaars M, Schomakers BV, Elfrink HL, et al. Metabolomics and lipidomics in *Caenorhabditis elegans* using a single-sample preparation. *Dis Model Mech*. 2021;14:dmm047746.
- Held NM, Buijink MR, Elfrink HL, et al. Aging selectively dampens oscillation of lipid abundance in white and brown adipose tissue. *Sci Rep*. 2021;11:5932.
- Herzog K, Pras-Raves ML, Vervaart MAT, et al. Lipidomic analysis of fibroblasts from Zellweger spectrum disorder patients identifies disease-specific phospholipid ratios. *J Lipid Res*. 2016;57:1447-1454.
- Los DA, Murata N. Structure and expression of fatty acid desaturases. *Biochim Biophys Acta*. 1998;1394:3-15.
- Park HG, Engel MG, Vogt-Lowell K, Lawrence P, Kothapalli KS, Brenna JT. The role of fatty acid desaturase (FADS) genes in oleic acid metabolism: FADS1 $\Delta 7$ desaturates 11-20:1 to 7,11-20:2. *Prostaglandins Leukot Essent Fatty Acids*. 2018;128:21-25.
- Violante S, IJlst L, Ruiten J, et al. Substrate specificity of human carnitine acetyltransferase: implications for fatty acid and branched-chain amino acid metabolism. *Biochim Biophys Acta*. 2013;1832:773-779.

24. Cinti DL, Cook L, Nagi MN, Suneja SK. The fatty acid chain elongation system of mammalian endoplasmic reticulum. *Prog Lipid Res.* 1992;31:1-51.
25. Kim, S., Chen, J., Cheng, T., Gindulyte, A., He, J., He, S., Li, Q., Shoemaker, B. A., Thiessen, P. A., Yu, B., Zaslavsky, L., Zhang, J., & Bolton, E. E. Fatty acid elongation in mitochondria. National Center for Biotechnology Information. PubChem Pathway Summary for Pathway SMP0000054 (2023). Available at: <https://pubchem.ncbi.nlm.nih.gov/pathway/PathBank:SMP0000054>. (Accessed: 29th December 2023)
26. Bakermans AJ, Geraedts TR, van Weeghel M, et al. Fasting-induced myocardial lipid accumulation in long-chain acyl-CoA dehydrogenase knockout mice is accompanied by impaired left ventricular function. *Circ Cardiovasc Imaging.* 2011;4:558-565.
27. van der Veen JN, Kennelly JP, Wan S, Vance JE, Vance DE, Jacobs RL. The critical role of phosphatidylcholine and phosphatidylethanolamine metabolism in health and disease. *Biochim Biophys Acta.* 2017;1859:1558-1572.
28. Lu Y-W, Claypool SM. Disorders of phospholipid metabolism: an emerging class of mitochondrial disease due to defects in nuclear genes. *Front Genet.* 2015;6:3.
29. Wortmann S, Rodenburg RJT, Huizing M, et al. Association of 3-methylglutaconic aciduria with sensori-neural deafness, encephalopathy, and Leigh-like syndrome (MEGDEL association) in four patients with a disorder of the oxidative phosphorylation. *Mol Genet Metab.* 2006;88:47-52.
30. Okazaki Y, Saito K. Roles of lipids as signaling molecules and mitigators during stress response in plants. *Plant J.* 2014;79:584-596.
31. Meyer Zu Heringdorf D, Jakobs KH. Lysophospholipid receptors: signalling, pharmacology and regulation by lysophospholipid metabolism. *Biochim Biophys Acta.* 2007;1768:923-940.
32. Kimura T, Jennings W, Epand RM. Roles of specific lipid species in the cell and their molecular mechanism. *Prog Lipid Res.* 2016;62:75-92.
33. Den Boer MEJ, Ijlst L, Wijburg FA, et al. Heterozygosity for the common LCHAD mutation (1528G>C) is not a major cause of HELLIP syndrome and the prevalence of the mutation in the Dutch population is low. *Pediatr Res.* 2000;48:151-154.
34. Merritt JL, MacLeod E, Jurecka A, Hainline B. Clinical manifestations and management of fatty acid oxidation disorders. *Rev Endocr Metab Disord.* 2020;21:479-493.
35. Yang J, Yuan D, Tan X, et al. Analysis of a family with mitochondrial trifunctional protein deficiency caused by HADHA gene mutations. *Mol Med Rep.* 2022;25:47.
36. Knuplez E, Marsche G. An updated review of pro- and anti-inflammatory properties of plasma lysophosphatidylcholines in the vascular system. *Int J Mol Sci.* 2020;21:4501.
37. Tan ST, Ramesh T, Toh XR, Nguyen LN. Emerging roles of lysophospholipids in health and disease. *Prog Lipid Res.* 2020;80:101068.
38. Law S-H, Chan ML, Marathe GK, Parveen F, Chen CH, Ke LY. An updated review of lysophosphatidylcholine metabolism in human diseases. *Int J Mol Sci.* 2019;20:1149.
39. Barendsen RW, Dijkstra IME, Visser WF, et al. Adrenoleukodystrophy newborn screening in The Netherlands (SCAN study): the X-factor. *Front Cell Dev Biol.* 2020;8:499.
40. Elizondo G, Matern D, Vockley J, Harding CO, Gillingham MB. Effects of fasting, feeding and exercise on plasma acylcarnitines among subjects with CPT2D, VLCADD and LCHADD/TFPD. *Mol Genet Metab.* 2020;131:90-97.
41. Czumaj A, Szrok-Jurga S, Hebanowska A, et al. The pathophysiological role of CoA. *Int J Mol Sci.* 2020;21:9057.
42. Naquet P, Kerr EW, Vickers SD, Leonardi R. Regulation of coenzyme A levels by degradation: the 'Ins and Outs'. *Prog Lipid Res.* 2020;78:101028.
43. Minaga T, Sharma ML, Kun E, Piper WN. Enzymatic degradation of succinyl-coenzyme A by rat liver homogenates. *Biochim Biophys Acta.* 1978;538:417-425.
44. Zatz M, Engelsens SJ, Markey SP. Biosynthesis of S-methyl-N-oleoylmercaptoethylamide from oleoyl coenzyme A and S-adenosylmethionine. *J Biol Chem.* 1982;257:13673-13678.
45. Hartig MB, Hörtnagel K, Garavaglia B, et al. Genotypic and phenotypic spectrum of PANK2 mutations in patients with neurodegeneration with brain iron accumulation. *Ann Neurol.* 2006;59:248-256.
46. Dusi S, Valletta L, Haack TB, et al. Exome sequence reveals mutations in CoA synthase as a cause of neurodegeneration with brain iron accumulation. *Am J Hum Genet.* 2014;94:11-22.
47. Li W-B, Shen NX, Zhang C, et al. Novel PANK2 mutations in patients with pantothenate kinase-associated neurodegeneration and the genotype-phenotype correlation. *Front Aging Neurosci.* 2022;14:848919.

SUPPORTING INFORMATION

Additional supporting information can be found online in the Supporting Information section at the end of this article.

How to cite this article: Schwantje M, Mosegaard S, Knottnerus SJG, et al. Tracer-based lipidomics enables the discovery of disease-specific candidate biomarkers in mitochondrial β -oxidation disorders. *The FASEB Journal.* 2024;38:e23478. doi:[10.1096/fj.202302163R](https://doi.org/10.1096/fj.202302163R)